1   **Experimental investigation of flow pattern and sediment deposition in**

2   **rectangular shallow reservoirs**

3   Matthieu DUFRESNE[1], Benjamin J. DEWALS[1,2], Sébastien ERPICUM[1], Pierre

4   ARCHAMBEAU[1] and Michel PIROTTON[1]

5

6   **Abstract**

7   This work involved the experimental investigation of flow pattern, preferential regions of

8   deposition and trap efficiency as a function of the length of rectangular shallow reservoirs.

9   Four flow patterns were identified (from longer to shorter reservoirs): an asymmetric flow

10 with two reattachment points, an asymmetric flow with one reattachment point, an unstable

11 flow, and a symmetric flow without any reattachment point. Using dye visualizations, the

12 median value and the temporal variability of the reattachment lengths were precisely

13 measured for the asymmetric flows. For each stable flow, sediment tests with plastic particles

14 were carried out. The regions of deposition on the bed of the reservoir were clearly a function

15 of the flow pattern. The transition from an asymmetric flow pattern to a symmetric flow

16 pattern was responsible for an abrupt decrease of the trap efficiency; a number of regression

17 laws were discussed to take it into account.

18

19 **Key Words:** Deposition, Flow patterns, Reservoirs, Sediment, Shallow water

20

21 **1 Introduction**

22 Tanks, basins, ponds, lagoons (called reservoirs below) are commonly used in hydraulic

23 engineering. Because of generally quiescent conditions, these works are conducive to the

---

[1] University of Liège (ULg), ArGEnCO department, MS²F sector, Hydrology, applied hydrodynamics and hydraulic constructions (HACH), Chemin des chevreuils, 1, bât B52/3, étage +1, 4000 Liège, Belgium. E-mail: matthieu.dufresne@free.fr, hach@ulg.ac.be

[2] Belgian fund for scientific research (F.R.S.-FNRS).

1   settling of particles. Therefore, reservoirs must be carefully designed according to the role

2   they will play. For example, sedimentation must be maximized in settling basins (stormwater

3   treatment, protection of irrigation or hydro-electric power structures, *etc*.) whereas it must be

4   minimized in storage facilities (irrigation, hydro-electric power generation, flood control,

5   *etc*.).

6

7   The prediction of deposition as a function of the geometry of the reservoir, the hydraulic

8   conditions and the sediment characteristics is still a great challenge. While empirical and

9   semi-empirical methods have been developed for the last sixty years to determine the amount

10   of deposits (see for example Jothiprakash and Garg 2008 for reservoirs, Garde *et al*. 1990,

11   Ranga Raju *et al*. 1999 for basins; Kowalski *et al*. 1999 for combined sewer detention tanks;

12   Luyckx *et al*. 1999 for high side weir overflows), they cannot determine their spatial

13   distribution, which is required to well define the sediment removal strategy. To get this

14   information, the knowledge of the flow pattern is a prerequisite. It is also questionable

15   whether the relative imprecision of these methods is not because they express the trap

16   efficiency of the reservoir (the ratio of the deposited mass to the incoming mass) without

17   taking into account the flow pattern.

18

19   Saul and Ellis (1992) highlighted that complex flow patterns take place in rectangular storage

20   tanks and that the flow pattern governs the sediment transport processes. Stovin and Saul

21   (1994) carried out experiments in a 2.00 m long and 0.97 m wide storage tank. The circular

22   inlet and outlet were respectively 0.19 m and 0.15 m in diameter. The water depth was about

23   0.20 m (the geometry was quasi bi-dimensional). The velocity in the inflow pipe was 0.56

24   m/s. Crushed olive stone was used as the model sediment (median grain size ≈ 0.050 mm,

25   density ≈ 1,500 kg/m^3). The writers showed that the flow field was characterised by a large

1   clockwise circulation and a small counter clockwise circulation in the upstream left corner of

2   the tank (asymmetric flow pattern); deposits were located in three preferential regions: in both

3   upstream corners of the tank and in the core of the large circulation zone. Varying the inflow

4   velocity (in the range $\approx 0.1 - 0.7$ m/s), Stovin and Saul (1996) proposed a linear relationship

5   between the percentage of the bed that is covered by deposits and the trap efficiency.

6

7   Kantoush et al. investigated the influence of the geometry of shallow reservoirs on flow

8   patterns and sedimentation by suspended sediments (Kantoush 2008, Kantoush *et al*. 2008).

9   His benchmark case was a 0.20 m high water flow entering a 6.00 m long and 4.00 m wide

10   reservoir by a 0.25 m wide channel at a velocity of 0.14 m/s. In this situation the main flow

11   was deflected on the right wall, leading to the formation of a large counter clockwise

12   circulation zone in the whole structure and a small clockwise circulation zone in the right inlet

13   corner (the jet may also be deflected on the left wall, depending on the experiment). Similar

14   patterns were observed when decreasing the breadth of the reservoir (3.00 m, 2.00 m, 1.00 m

15   and 0.50 m for which the flow was fully reattached in the downstream zone of the reservoir).

16   Asymmetry disappeared when decreasing the length of the reservoir (5.00 m, 4.00 m, and

17   3.00 m). For these geometries, the jet was not deflected at entrance in the reservoir, leading to

18   the formation of two large symmetric circulation zones. The writer used crushed walnut shells

19   (median grain size ≈ 0.050 mm, density $\approx 1,500$ kg/m^3) to study morphological evolution.

20   Nevertheless, the flow pattern was not steady during sediment tests, probably because of the

21   large amount of deposits near the inlet of the reservoir (these deposits led to change the

22   direction of the jet entering the basin during experiments).

23

24   A number of experimental studies were conducted in more complex geometries. Modifying

25   the basic chamber configuration described above, Stovin (1996) highlighted some effects of

1   the gradient benching and the length to breadth ratio on sediment distribution. Dufresne *et al*.

2   (2009) showed that flow and sediment distribution became quasi-symmetric when increasing

3   the water level above the top of the inlet pipe. The influence of columns and obstacles (a wall

4   located in front of the inlet) on sediment deposition was also investigated (Dufresne 2008).

5

6   This study focuses on rectangular shallow reservoirs, as illustrated in Figure 1. Here, L =

7   length of the reservoir; B = breadth of the reservoir; b = breadth of the inlet and outlet

8   channels; ΔB = lateral expansion; h = water depth; and U = inflow velocity. The aim of this

9   work is firstly to investigate the preferential regions of deposition for the main flow patterns

10   that can take place in rectangular shallow reservoirs; secondly, to study the influence of the

11   flow pattern on the trap efficiency.

12

13   **2 Experimental investigation**

14   2.1 Experimental set-up

15   The experiments were carried out at the engineering hydraulics laboratory of the University of

16   Liège, Belgium. The experimental set-up diagrammatically shown in Figure 1 consisted of a

17   10.40 m long and 0.985 m wide glass channel in which blocks can be arranged to build

18   different geometries of rectangular reservoirs. The base of the flume was horizontal.

19

20   The flow entered the channel from a stilling basin through a porous screen in order to prevent

21   fluctuations in water level and make the velocity field uniform. The flow was then contracted

22   to the desired breadth of the inlet channel (b) in a converging section with circular shape; the

23   inlet section of the reservoir (with straight parallel walls) was 2.00 m long. At the entrance of

24   the reservoir, the flow suddenly expanded to the breadth of the reservoir (B). At the exit of the

25   reservoir, the flow suddenly contracted to the outlet channel breadth (b). The outlet channel

1   was 1.00 m long; its downstream boundary corresponded to a gate (to control the water level)

2   and a waterfall. All the surfaces were made of glass, except the two parallel walls of the inlet

3   and outlet channels (PVC) and the converging section (metallic sheets). In this study, the

4   lateral expansion equaled 0.350 m. Three lengths were investigated: 1.80, 2.20 and 7.00 m;

5   they were chosen after trial and error so that different flow patterns could be observed

6   (symmetric flow, asymmetric flow with one reattachment point and asymmetric flow with

7   two reattachment points).

8

9   The volumetric flow rate was measured with an electromagnetic flowmeter upstream of the

10   flume; it was also measured with a triangular weir in the water collection channel downstream

11   of the waterfall in order to enhance accuracy on small values. Water depth in the reservoir

12   was measured with a level meter in the middle of the breadth 0.10 m downstream of the

13   entrance of the reservoir and 0.10 m upstream of the exit of the reservoir. The maximum

14   difference between the two values was 0.002 m. Therefore only the upstream value is reported

15   hereafter.

16

17   2.2 Sediment

18   Granular plastic (Styrolux 656 C) was chosen as the model sediment. The particles were

19   elliptical cylinders with a density of 1020 kg/m^3 (given by the producer BASF). We randomly

20   selected 30 particles and measured their dimensions using a Vernier caliper, and their fall

21   velocities in a water column. The results show that the sediment characteristics are relatively

22   uniform (see Table 1). Based on these measurements, 2.4 mm (cube root of the mean volume)

23   was chosen as the characteristic sediment size; 25 mm/s, as the characteristic fall velocity.

24

25   2.3 Experimental procedure

1 After preliminary sediment tests, one single inflow velocity was chosen for all the

2 experiments (0.28 m/s). This velocity was sufficiently high to avoid deposition in the inlet

3 channel and near the entrance of the reservoir (in order to avoid modifications of the direction

4 of the incoming jet), and sufficiently low to allow deposition in the reservoir.

5

6 Two kinds of experiments were carried out. The first one consisted in flow tests; their aim

7 was to describe (qualitatively and quantitatively) the flow pattern. The second one consisted

8 in sediment tests; their aim was to describe the spatial distribution of deposits and the trap

9 efficiency of the reservoir. The experimental conditions are given in Table 2 (flow tests) and

10 Table 3 (sediment tests). Here, U = velocity in the inlet channel; ρ = water density; μ = water

11 viscosity; g = gravitational acceleration; u_* = shear velocity; ρ_s = sediment density, d =

12 sediment size; w = sediment fall velocity; and q_s = sediment discharge. The uncertainty was

13 about 0.002 m in the water depth (level meter) and about 0.01 m/s in the velocity (based on

14 uncertainties in discharge and water depth). The water temperature was between 18 and 20°C,

15 depending on the experiment. In order to check the reproducibility, all the experiments were

16 repeated (except test F15-a for which the flow did not stabilize). Successive tests are named

17 "a", "b", etc.

18

19 2.4 Flow tests

20 Visual investigations employing dye injections disclosed the flow pattern: symmetry or

21 asymmetry, number of circulation zones, approximate locations of reattachment points.

22 Despite steady boundary conditions, a wake zone (characterized by unsteadiness) took place

23 downstream of the entrance of the reservoir. Therefore, successive dye injections were

24 generally needed to describe a "mean" behavior.

25

1   The reattachment is defined as the point upstream of which the longitudinal velocity is

2   negative (from downstream to upstream) and downstream of which the longitudinal velocity

3   is positive (from upstream to downstream). Because of the unsteadiness of the flow, Chu et al.

4   (2004) proposed to define it as "the point where the movements to the upstream and

5   downstream directions are equally probable" (this definition corresponds to the median

6   reattachment). To our knowledge, only the median position has been reported in the literature,

7   using for example visualization of displacement of confetti on the water surface (Babarutsi *et*

8   *al.* 1989, Babarutsi and Chu 1991, Chu *et al.* 2004). Only Abbott and Kline (1962)

9   characterized the fluctuations of the reattachments lengths by taking a large number of points

10 (see for example Figures 11 and 12 of their paper: the writers showed a band of two

11 regression curves instead of a single one). In the present study, we better characterized these

12 fluctuations by determining the velocity distribution along the wall near the median

13 reattachment. Preliminary tests allowed us to define the following protocol.

14

15 Once the reattachment had been roughly located by dye visualization, the method consisted in

16 injecting drops of dye at various points against the wall near the reattachment point. In each

17 point, 100 drops of dye were injected at a frequency of one drop every 2 seconds; for each

18 drop, the sense of the flow was observed by eye. A displacement of the dye from upstream to

19 downstream corresponded to a positive velocity whereas a displacement from downstream to

20 upstream corresponded to a negative velocity. The number of injected drops (100) and the

21 duration of measurement (100 times 2 seconds) were chosen after preliminary tests to ensure

22 a statistically meaningful result. Since the objective of this work is the study of deposits, the

23 reattachment lengths were measured near the bottom of the reservoir (0.04 m above the bed).

24 Nevertheless, "reasonable" two-dimensionality of the flow was always checked by dye

25 visualization.

1

2 A 95% confidence interval of the proportion of negative velocities was calculated using a

3 small sample method in order to estimate the "uncertainty" of each measurement (see

4 Wonnacott and Wonnacott 1977, p. 224). The 95% confidence intervals of the median

5 reattachment lengths were determined using interpolations of the upper-bounds and lower-

6 bounds of the confidence intervals between locations for which the proportions are closest to

7 50%. The 95% confidence intervals of the median reattachment lengths are given in Table 2

8 (R_1 and R_2 for respectively the shorter one and the longer one).

9

10 Another piece of information was extracted from these measurements: the reattachment

11 lengths fit a normal distribution. By minimizing the sum of the differences between the

12 measured and the normal proportions in square, the mean, μ, and the standard deviation, σ, of

13 a Gaussian distribution were determined. These values are also given in Table 2.

14

15 Table 4 summarizes the flow conditions in a dimensionless form. Based on dimensional

16 analysis and literature, six dimensionless flow parameters govern the flow pattern: the

17 dimensionless length (ratio of the length to the lateral expansion), the lateral expansion ratio

18 (ratio of the lateral expansion to the breadth of the inlet channel), the vertical confinement

19 (ratio of the lateral expansion to the water depth), the Reynolds number, the Froude number,

20 and the bed friction number (see Table 4). Here, c_f is the bed friction coefficient; it was

21 estimated using the formula recommended by the ASCE task force on friction factor in open

22 channel flow (see Henderson 1966, p. 95). The bed friction coefficient was used to estimate

23 the shear velocity too. Instead of the lateral expansion ΔB, the breadth B could have been used

24 as the representative lateral dimension of the reservoir.

25

1 In order to allow asymmetric flow patterns to develop in long basins, a lateral expansion ratio

2 greater than 0.25 was chosen (see Abbott and Kline 1962 about "infinitely" long reservoirs).

3 The vertical confinement was chosen sufficiently low to avoid friction effect: the friction had

4 probably no influence on the flow pattern since 0.003 is small compared to the critical values

5 highlighted in the literature (0.05 – 0.10 for unilateral expansions, see Chu *et al*. 2004). The

6 dimensionless lengths were chosen by trial and error in order to find the transition between

7 asymmetric and symmetric flows. Based on preliminary tests about sediment transport (see

8 above), a Froude number of 0.20 was chosen. The range of Reynolds numbers shows that the

9 flows were fully turbulent.

10

11 2.5 Sediment tests

12 In order to avoid flocculation, the plastic sediment was wet prior to experiment. It was input

13 into the inflow 2.00 m upstream of the entrance of the reservoir. The injection consisted in

14 discrete batches of 80 g (dry mass) over 10 second time intervals. The total period of injection

15 was 10 minutes for each experiment. The inflow concentration was 0.50 g/L. Based on

16 uncertainties in discharge, sediment mass and time period, the uncertainty in the inflow

17 concentration was about 0.02 g/L.

18

19 Using a net, particles were collected in the waterfall downstream of the reservoir in three time

20 periods: between 2 and 4 minutes after the beginning of the injection, between 5 and 7

21 minutes, and between 8 and 10 minutes. Each sample was dried and weighted, so that the

22 mean outflow concentration could be calculated for the three time intervals. The trap

23 efficiency, η, was calculated for each period using Equation 1. Here, c_{in} = inflow

24 concentration; c_{out} = outflow concentration.

25 $\eta = \dfrac{c_{in} - c_{out}}{c_{in}}$ (1)

1   The uncertainty in the outflow concentration was between 0.005 and 0.020 g/L (depending on

2   the outflow concentration), which leads to an absolute uncertainty in the efficiency of 10% –

3   15% (0.10 – 0.15).

4

5   For each experiment, the bed of the reservoir was filmed over time in order to monitor the

6   deposits. The spatial distributions of deposits given below are based on these movies.

7

8   Table 5 summarizes the dimensionless sediment parameters: the dimensionless bed shear

9   stress, the particle Reynolds number (calculated with the shear velocity), the dimensionless

10 fall velocity (ratio of the fall velocity to the shear velocity), and the dimensionless solid

11 discharge. Observations by eye showed that bed-load and suspended load coexisted in the

12 inlet channel (the dimensionless fall velocity was about 2). However, bed-load was the

13 predominant mode of transport in the reservoir.

14

15 **3 Results**

16 3.1 Flow patterns

17 Dye visualizations highlighted four different flow patterns. They are reported in Tables 2 and

18 3.

19

20 When the length of the reservoir was 1.80 m, the flow presented a symmetric behavior, as

21 illustrated in Figure 3 (pattern S0). The jet went in a straight way from the entrance to the exit

22 of the reservoir; two symmetric circulation zones took place in the reservoir. It was also

23 observed that the counter-currents detached from the wall approximately 0.3 m downstream

24 of the inlet section of the reservoir, leading to the formation of a small circulation zone in

25 each upstream corner. This zone was not drawn as a two-dimensional circulation in Figure 3

1   because dye visualization highlighted three-dimensional effects (vertical eddies); this

2   behavior is consistent with the observations of Abbott and Kline (1962).

3

4   Symmetry disappeared when increasing the length of the reservoir to 2.20 m. The jet was

5   deflected on one side of the reservoir. It reattached the wall after a distance named R_1 in figure

6   3, which led to the formation of a large circulation zone. A smaller circulation zone took place

7   upstream of the reattachment. This flow pattern is denoted by "A1".

8

9   For intermediate length (2.00 m), the flow did not stabilize in spite of steady boundary

10   conditions: it fluctuated between a symmetric behavior (S0) and an asymmetric behavior

11   (A1). The fluctuations between these two patterns were not periodic and seemed to be

12   completely random. This type of flow is reported as "A1/S0" in Table 2. Even if the flow was

13   unsteady in this situation, it was completely different from the meandering jet (periodic

14   behavior) observed by Kantoush (2008) when decreasing the water depth below 0.20 m.

15

16   For the longest reservoir (7.00 m), the flow still remained asymmetric. As for a length of 2.20

17   m, the flow reattached on one side of the reservoir after a distance R_1 but also possibly on the

18   opposite wall after a distance R_2. In this situation, the flow was fully reattached in the

19   downstream zone of the basin (all the x-velocities in a transversal section are positive).

20   Successive dye visualizations showed that the longer reattachment was highly unsteady, and

21   sometimes completely missing. This third stable pattern is illustrated in Figure 3 (A2).

22

23   These results highlight a transition between symmetric and asymmetric flows for a

24   dimensionless length in the range 5.1 – 6.3 (the flow was symmetric below and asymmetric

25   above). This critical range is different from the results of the experiments carried out by

1   Kantoush (2008) for which the transition occurred for a dimensionless length in the range

2   2.7 – 3.2. This shows that the dimensionless length is not sufficient to predict the flow

3   pattern; additional dimensionless parameters from Table 4 are needed. There have been

4   several attempts to define a criterion for forecasting the flow pattern in rectangular shallow

5   reservoirs, from the simplest length to breadth ratio (Kantoush 2007) to more complex criteria

6   involving the length of the reservoir, its breadth (eventually the lateral expansion) and the

7   breadth of the inlet channel (Kantoush 2008, Dewals et al. 2008, Dufresne 2008). Among

8   these criteria, only the one defined in Equation (2) and based on numerical simulations of

9   Dufresne (2008) is consistent with the two experimental campaigns. Indeed, the range

10   corresponding to the transition highlighted by Kantoush (2.2 – 2.6) partially overlaps the

11   range highlighted in the present study (2.3 – 2.9). Moreover, these two ranges are consistent

12   with the critical value that Dufresne (2008) recommended: symmetric flows below 2.36 and

13   asymmetric flows above 2.36.

14   $$A_L = \frac{L}{B}\left(\frac{B}{b}\right)^{0.2} = \frac{L}{B^{0.8}b^{0.2}} \qquad (2)$$

15   Nevertheless, the relatively close hydraulic conditions of the two campaigns raise the question

16   of the validity of this geometrical criterion in more general situations (various water depths

17   and various velocities). Further investigations varying the lateral expansion ratio, the vertical

18   confinement and the Froude number are currently in progress in order to find a general

19   criterion.

20

21   3.2 Reattachment lengths

22   Figures 4 and 5 display the negative velocity distributions near reattachment for the

23   experimental condition F4 (tests "a" and "c"), which corresponds to the flow pattern A2.

24   Using these figures, the median reattachment length and the range of fluctuation of the

25   reattachment length can be precisely determined. In Table 2, the median reattachment length

1   is given using a 95% confidence interval (measurement uncertainty); the range of fluctuation

2   is given using the mean and the standard deviation of a Gaussian distribution (temporal

3   variability). From Figure 4, we are for example 95% confident that the median reattachment

4   length R_1 of experiment F4-a was between 1.16 and 1.21 m. Using the normal distribution,

5   one can also extract that the reattachment length was between 1.05 and 1.31 m during 80% of

6   the time; it was smaller than 1.05 m during 10% of the time, and greater than 1.31 m during

7   10% of the time.

8

9   The comparison between Figures 4 and 5 highlights the different nature of the two

10   reattachments. Whereas the first one was rather steady over time (standard deviation about

11   0.10 m), the second one was highly unsteady (2.1 m), which means that it fluctuated over a

12   long distance on the wall of the reservoir. Here, it must be precised that the distribution of the

13   negative velocities of the second reattachment is not rigorously normal (one can see in Figure

14   5 that the distribution of the second reattachment length is truncated by the downstream wall

15   of the reservoir). Nevertheless, we also describe the second reattachment using the mean and

16   the standard deviation of a Gaussian law in order to make possible comparison between R_1

17   and R_2. At a distance of 6.5 m from the entrance, the proportion of negative velocities was

18   close to 50%, which means that the reattachment completely disappeared during about half

19   the time (the length of the reservoir is 7.00 m). Therefore, the instantaneous flow fluctuated

20   between A1 and A2 while the median flow was A2, which is consistent with previous dye

21   visualizations (the second reattachment was sometimes missing). The high unsteadiness of the

22   second reattachment length was also highlighted by Abbott & Kline (1962) about flow over

23   backward facing steps.

24

1   The median reattachment length R_1 measured for the experimental condition F14 was a little

2   bit smaller than the value measured for F4 (1.04 – 1.10 m and 1.03 – 1.06 m instead of 1.16 –

3   1.21 m and 1.15 – 1.18 m), which may be interpreted as an effect of the longitudinal

4   confinement. Nevertheless, it can be said that the flow patterns A1 and A2 are quasi-identical

5   in the upstream zone of the reservoir (same order of magnitude for the median position and

6   the variability of the reattachment). They only significantly differ in the downstream zone of

7   the reservoir.

8

9   It can be noticed that the median reattachment length of the "last" asymmetric flow before the

10   transition to symmetric pattern was approximately equal to half the length of the reservoir

11   (1.04 – 1.10 and 1.03 – 1.06 m compared to 2.20 m). This behavior was similar in the

12   experiments of Kantoush (2008): the writer showed that when the breadth of the reservoir

13   equaled 4.00 m, the transition occurred between the lengths 5.00 and 6.00 m; the mean

14   reattachment length for a length of 6.00 m was ≈ 2.65 m (see Figure 4.16 of his thesis).

15

16   3.3 Spatial distribution of deposits

17   Figure 6 displays the preferential zones of deposition for the three stable flow patterns after

18   10 minutes of sediment input (a clear pattern of deposition was observed after 4 – 5 minutes

19   for all the sediment tests). Since the borders of the deposition zones slightly evolved over time

20   (because of the unsteadiness of the flow), Figure 6 is only a sketch of the deposits at a given

21   "time" (it is representative of a few seconds). The comparison between grey zones (tests a)

22   and dotted lines (tests b) exhibits the same general shape of deposits.

23

24   From this figure, it can be concluded that the location of the deposits is clearly a function of

25   the flow pattern. When the length was 1.80 m (flow pattern S0), the pattern of sediment

1   deposition was quasi-symmetric: deposition took place in each inlet corners. The size of the

2   deposition regions was approximately a few centimeters to 0.3 m in width and 0.4 – 0.8 m in

3   length. The shape of the downstream part of these zones was elongated and corresponded to

4   deposits regularly eroded (wake zone).

5

6   Like the flow pattern, the pattern of sediment deposition became asymmetric when increasing

7   the length. When the reservoir was 2.20 m long (flow pattern A1), three regions of deposition

8   took place on the bed: the two inlet corners and the core of the large circulation zone. Here,

9   the jet was deflected on the right wall of the reservoir. Despite its relatively small area (about

10   0.6 m long and 0.2 m wide), the zone of deposition in the core of the large circulation zone

11   contained the largest amount of deposits. After 10 minutes of injection, the thickness of

12   particles was about 20 mm (several layers of particles) while it was less than 5 mm in the

13   others zones. In this zone, the deposits were regularly eroded due to the relative unsteadiness

14   of the flow, but they remained captured in the circulation current and escaped only by

15   intermittent "bursts". In the right inlet corner, the region of deposition was about 0.4 m long

16   and 0.2 – 0.3 m wide. As for the 1.80 m long reservoir, the downstream part of this region

17   was regularly eroded because of the wake. The left inlet corner region consisted of very

18   scattered deposits that were brought by the current from downstream to upstream. Regularly,

19   the first and the third regions were connected by a narrow band of (intermittent) deposits (see

20   dotted lines).

21

22   When the length was 7.00 m (flow pattern A2), two main zones of deposition were identified.

23   As for the flow pattern A1, a first region took place in the right inlet corner (the jet was

24   deflected to the right). A second region of deposition took place mainly in the downstream

25   zone of the reservoir. Its length was about 6.0 m and its width varied between a few

1 centimeters to approximately 0.4 – 0.6 m in its downstream part. Probably because of the

2 unsteadiness of the flow in this zone (fluctuations of the longer reattachment length), the

3 deposits were regularly eroded. This region of deposition was quasi-symmetric in the

4 downstream part of the reservoir (where the flow was fully reattached). Contrarily to the

5 experimental condition ST2, there was no region of deposition in the left inlet corner of the

6 reservoir. This can be explained by the fact that the current from downstream to upstream that

7 took place in this zone contained a small amount of particles (they settled or escaped before

8 being brought back to the upstream zone of the reservoir).

9

10 3.4 Trap efficiency

11 As shown in Table 3, the efficiencies η_1, η_2 and η_3 (corresponding to the three time periods)

12 are scattered for a given length. Different reasons explain this behavior: the time needed by

13 the particles to travel between the inlet and the outlet (one can see that 2 minutes were not

14 sufficient to get "equilibrium" between the inflow and the outflow concentrations when the

15 length was 7.00 m), the uncertainty of the measurements (10% – 15%), and the natural

16 variability (although the equilibrium is reached, the difference between η_3 obtained for ST1-a

17 and ST1-b is greater than the uncertainty). The first reason leads to reject the η_1 values as

18 meaningful efficiencies for the longest reservoir whereas the η_2 and η_3 values and all the

19 efficiencies obtained for the other lengths are considered hereafter.

20

21 The natural variability was probably due to the unsteadiness of the flow, the unsteadiness of

22 the sediment input (discrete batches) and also the nature of sediment transport itself,

23 especially because bed-load was predominant. Indeed, Böhm et al. (2004) showed that even

24 under well-controlled experimental conditions and despite steady supply, solid discharge

25 exhibits significant variations with time. One explanation given by the writers was the

1   collective entrainment of deposited particles, which was observed during our own

2   experiments. This physical variability leads to define some ranges of efficiency rather than

3   single values. Table 6 shows these approximate ranges as a function of the length of the

4   reservoir. In this table, both uncertainty and variability are taken into account.

5

6   The influence of the length of the reservoir on the efficiency is illustrated in Figure 7. It can

7   be seen that the decrease of the efficiency between 2.20 and 1.80 m is the same order of

8   magnitude as the decrease between 7.00 and 2.20 m (about 20% – 25%). Therefore, the

9   transition from an asymmetric flow to a symmetric flow is responsible for a break in the

10   efficiency curve of the reservoir.

11

12   Even if the flow patterns observed for a length of 7.00 m and a length of 2.20 m were very

13   similar, it is interesting to notice that the nature of deposition seemed to be different, probably

14   because the particles were jailed in the circulation current for experiments ST2-a and ST2-b.

15   Based on the sketches of the experimental deposits (Figure 6), the areas of deposition were

16   estimated. Whereas the area of deposition was about 0.3 m^2 for a length of 2.20 m, it was

17   around 1.9 m^2 (six times bigger) for a length of 7.00 m. In the same time, the efficiency only

18   increases from the range 10% – 40% to 30% – 60%. One explanation is that the particles are

19   concentrated in the center of the circulation zone for the flow pattern A1 (as "jailed" by the

20   flow) whereas they are much dispersed for the flow pattern A2.

21

22   Although the number of points is too low and the values too scattered to propose a final

23   relationship between the length of the reservoir and the efficiency, assumptions can be made

24   and discussion is open. To do so, it can be added that the efficiency should tend towards zero

25   when decreasing the length. But the efficiency does not necessarily tend towards 100% when

1   increasing the length (even if it is fully reattached, the flow may be able to carry a non-zero

2   solid discharge because of the relatively small breadth of the flume).

3

4   Exponential laws were often proposed as efficiency relationships (Sumer 1977 cited by Garde

5   et al. 1990, Garde et al. 1990, Ranga Raju and Kothyari 2004 for settling basins; Luyckx et al.

6   1999 for the parameters of the efficiency relationship of a high side weir overflow). In this

7   study, contrarily to the cited relationships, the constant L_0 of such a law (see Equation 3) must

8   be different from zero to accurately reproduce the abrupt change around the transition; this

9   parameter is the length for which the efficiency becomes zero. The two other constants are η_0,

10   a maximum efficiency (for infinitely long reservoir) and α, the inverse of a characteristic

11   length (to represent the spread of the curve). This exponential relationship leads to negative

12   values when the length is lower than L_0; therefore, the expression is replaced by zero in this

13   situation.

14   $$\eta = 0\% \quad \text{if } L \leq L_0$$
$$\eta = \eta_0 \left(1 - e^{-\alpha(L-L_0)}\right) \quad \text{if } L \geq L_0 \qquad (3)$$

15   The inconvenience of such a law is that the constant L_0 has no meaning in relation to the flow

16   pattern. A sigmoid law (as written in Equation 4) is more relevant to highlight the transition

17   between symmetric and asymmetric flows in the efficiency relationship. Here, the constants

18   of the law are a maximum efficiency, η_0, the inverse of a characteristic length, α, and a critical

19   length, L_0. This last parameter is the length for which the transition between asymmetry and

20   symmetry occurs and is therefore between 1.80 and 2.20 m.

21   $$\eta = \frac{\eta_0}{1 + e^{-\alpha(L-L_0)}} \qquad (4)$$

22   The exponential law, the sigmoid law and two linear relationships (comparable slopes but

23   different intercept points) are illustrated in Figure 7; all of them reproduce the general shape

24   of the experimental data.

1

2 The laws described above are some possibilities for taking into account the transition between

3 symmetric and asymmetric flow patterns in a single efficiency relationship, but it is perhaps

4 unrealistic to seek such a goal. In this case, the only way would be to use different regression

5 laws depending of the flow pattern.

6

7 **4 Conclusions**

8 The objective of this work was to investigate the influence of the flow pattern on preferential

9 regions of deposition and trap efficiency in rectangular shallow reservoirs. The great

10 flexibility of the experimental set-up allowed easily changing the length of the reservoir and

11 precisely determining the transition between symmetric and asymmetric flow patterns.

12

13 Four flow patterns were identified (from longer to shorter reservoirs): an asymmetric flow

14 with two reattachment points (A2), an asymmetric flow with one reattachment point (A1), an

15 unstable flow (A1/S0), and a symmetric flow without any reattachment point (S0). Using dye

16 visualizations, the median value and the temporal variability of the reattachment lengths were

17 precisely measured for the asymmetric flow patterns A1 and A2.

18

19 For each stable flow, sediment tests with plastic particles were carried out. The regions of

20 deposition on the bed of the reservoir were mapped; they were clearly a function of the flow

21 pattern. The transition between symmetric to asymmetric flow patterns was responsible for an

22 abrupt increase in the efficiency curve. We discussed a number of regression laws to take it

23 into account.

24

Further investigations are currently in progress in order to find forecasting criteria of the flow pattern varying the dimensionless length, the lateral expansion ratio, the vertical confinement and the Froude number. Based on this work, the data about trap efficiency available in literature should be reanalyzed in order to better define efficiency relationships.

References

Abbott D. E. and Kline S. J. 1962, Experimental investigation of subsonic turbulent flow over single and double backward facing steps. Journal of Basic Engineering, Vol. 84, pp. 317-325.

Babarutsi S. and Chu V. H. 1991, Dye-concentration distribution in shallow recirculating flows. Journal of Hydraulic Engineering, Vol. 117, No. 5, pp. 643-659.

Babarutsi S., Ganoulis J. and Chu V. H. 1989, Experimental investigation of shallow recirculating flows. Journal of Hydraulic Engineering, Vol. 115, No. 7, pp. 906-924.

Böhm T., Ancey C., Frey P., Reboud J.-L. and Ducottet C. 2004, Fluctuations of the solid discharge of gravity-driven particle flows in a turbulent stream. Physical Review E, Vol. 69, No. 6, pp. 061307:1-13.

Chu V. H., Liu F. and Altai W. 2004, Friction and confinement effects on a shallow recirculating flow. Journal of Environmental Engineering and Science, Vol. 3, pp. 463-475.

1   Dewals B. J., Kantoush S. A., Erpicum S., Pirotton M. and Schleiss A. J. 2008, Experimental

2   and numerical analysis of flow instabilities in rectangular shallow basins. Environmental

3   Fluid Mechanics, Vol. 8, pp. 31-54

4   Dufresne M. 2008, La modélisation 3D du transport solide dans les bassins en

5   assainissement : du pilote expérimental à l'ouvrage réel. PhD thesis, Université Louis

6   Pasteur, Strasbourg, France (in French).

7   Dufresne M., Vazquez J., Terfous A., Ghenaim A. and Poulet J.-B. 2009, Experimental

8   investigation and CFD modelling of flow, sedimentation, and solids separation in a

9   combined sewer detention tank. Computers & Fluids, Vol. 38, No. 5, pp. 1042-1049.

10   Garde R. J., Ranga Raju K. G. and Sujudi A. W. R. 1990, Design of settling basins. Journal of

11   Hydraulic Research, Vol. 28, No. 1, pp. 81-91.

12   Henderson F. M. 1966, Open channel flow, Macmillan Series in Civil Engineering, Prentice

13   Hall.

14   Jothiprakash V. and Garg V. 2008, Re-look to conventional techniques for trapping efficiency

15   estimation of a reservoir. International Journal of Sediment Research, Vol. 23, No. 1,

16   pp. 76-84.

17   Kantoush S. A., Bollaert E. and Schleiss A. J. 2008, Experimental and numerical modelling of

18   sedimentation in a rectangular shallow basin. International Journal of Sediment Research,

19   Vol. 23, no. 3, pp. 212-232.

20   Kantoush S. A. 2008, Experimental study on the influence of the geometry of shallow

21   reservoirs on flow patterns and sedimentation by suspended sediments. PhD thesis, Ecole

22   Polytechnique Fédérale de Lausanne, Switzerland.

23   Kantoush S. A. 2007, Symmetric or asymmetric flow patterns in shallow rectangular basins

24   with sediment transport. Proceedings of the 32nd Congress of IAHR, "Harmonizing the

25   Demands of Art and Nature in Hydraulics", Venice, Italy.

1   Kowalski R., Reuber J. and Köngeter J. 1999, Investigations into and optimisation of the

2   performance of sewage detention tanks during storm rainfall events. Water Science and

3   Technology, Vol. 39, No. 2, pp. 43-52.

4   Luyckx G., Vaes G. and Berlamont J. 1999, Experimental investigation on the efficiency of a

5   high side weir overflow. Water Science and Technology, Vol. 39, No. 2, pp. 61-68.

6   Ranga Raju K. G. and Kothyari U. C. 2004, Sediment management in hydroelectric projects.

7   Proceedings of the 9th International Symposium on River Sedimentation, Yichang, China.

8   Ranga Raju K. G., Kothyari U. C., Srivastav S. and Saxena M. 1999, Sediment removal

9   efficiency of settling basins. Journal of Irrigation and Drainage Engineering, Vol. 125,

10   No 5, pp. 308-314.

11   Saul A. and Ellis D. 1992, Sediment deposition in storage tanks. Water Science and

12   Technology, Vol. 25, No. 8, pp. 189-198.

13   Stovin V. R. 1996, The prediction of sediment deposition in storage chambers base on

14   laboratory observations and numerical simulation. PhD thesis, University of Sheffield,

15   United Kingdom.

16   Stovin V. R. and Saul A. J. 1996, Efficiency prediction for storage chambers using

17   computational fluid dynamics. Water Science and Technology, Vol. 33, No. 9, pp. 163-170.

18   Stovin V. R. and Saul A. J. 1994, Sedimentation in storage tank structures. Water Science and

19   Technology, Vol. 29, No. 1-2, pp. 363-372.

20   Sumer B. 1977, Settlement of solid particles in open-channel flow. Journal of the Hydraulics

21   Division, Vol. 103, No. 11, pp. 1323-1337.

22   Wonnacott T. and Wonnacott R. 1977, Introductory statistics, Third edition, John Wiley &

23   Sons.

24

25

1 **Tables**

2

	Minimum value	Mean value	Maximum value
Height [mm]	2.30	2.55	2.85
Major axis [mm]	2.30	2.65	3.00
Minor axis [mm]	1.85	2.10	2.30
Density [kg/m^3]	-	1020 (given by BASF)	-
Fall velocity [mm/s]	20	25	30

3 Table 1. Features of the particles.

Test ID	ΔB [m]	b [m]	L [m]	h [m]	U [m/s]	Flow pattern	R_1 [m] (95% confidence interval)	μ_1 [m]	σ_1 [m]	R_2 [m] (95% confidence interval)	μ_2 [m]	σ_2 [m]
F4-a	0.350	0.285	7.000	0.201	0.28	A2	1.16 – 1.21	1.18	0.10	-	-	-
F4-b	0.350	0.285	7.000	0.200	0.29	A2	1.15 – 1.18	1.16	0.06	-	-	-
F4-c	0.350	0.285	7.000	0.203	0.27	A2	-	-	-	6.0 – 6.5	6.4	2.1
F14-a	0.350	0.285	2.200	0.205	0.27	A1	1.04 – 1.10	1.07	0.09	Ø	Ø	Ø
F14-b	0.350	0.285	2.200	0.207	0.28	A1	1.03 – 1.06	1.05	0.06	Ø	Ø	Ø
F15-a	0.350	0.285	2.000	0.204	0.27	A1/S0	-	-	-	Ø	Ø	Ø
F16-a	0.350	0.285	1.800	0.206	0.27	S0	Ø	Ø	Ø	Ø	Ø	Ø
F16-b	0.350	0.285	1.800	0.204	0.27	S0	Ø	Ø	Ø	Ø	Ø	Ø

Table 2. Summary of flow test conditions and main results ("-" for "non-measured", "Ø" for "does not exist").

Test ID	ΔB [m]	b [m]	L [m]	h [m]	U [m/s]	Flow pattern	C_{in} [g/L]	η_1	η_2	η_3
ST1-a	0.350	0.285	7.000	0.199	0.28	A2	0.50	73%	49%	57%
ST1-b	0.350	0.285	7.000	0.196	0.28	A2	0.50	69%	50%	34%
ST2-a	0.350	0.285	2.200	0.200	0.28	A1	0.50	26%	18%	36%
ST2-b	0.350	0.285	2.200	0.197	0.29	A1	0.50	31%	28%	32%
ST3-a	0.350	0.285	1.800	0.204	0.27	S0	0.51	13%	2%	7%
ST3-b	0.350	0.285	1.800	0.207	0.27	S0	0.50	9%	1%	6%

Table 3. Summary of sediment test conditions and main results.

Dimensionless parameter	Value(s)
$\dfrac{L}{\Delta B}$	5.1, 5.7, 6.3 and 20.0
$\dfrac{\Delta B}{b}$	1.23
$\dfrac{\Delta B}{h}$	between 1.69 and 1.78
$\dfrac{4\rho U h}{\mu}$	between 210,000 and 228,000
$\dfrac{U}{\sqrt{gh}}$	between 0.19 and 0.21
$\dfrac{c_f \Delta B}{2h}$	≈ 0.003

Table 4. Dimensionless flow parameters.

Dimensionless parameter	Value
$\dfrac{\rho u_*^2}{(\rho_s - \rho)gd}$	≈ 0.3
$\dfrac{\rho u_* d}{\mu}$	≈ 30
$\dfrac{w}{u_*}$	≈ 2
$\dfrac{q_s}{\sqrt{\left(\dfrac{\rho_s}{\rho}-1\right)gd^3}}$	≈ 0.5

Table 5. Dimensionless sediment parameters.

Length [m]	Trap efficiency
1.80	0% – 20%
2.20	10% – 40%
7.00	30% – 60%

Table 6. Ranges of trap efficiencies varying the length of the reservoir.
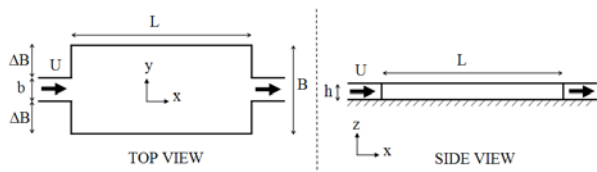
Fig. 1. Schemes of a rectangular shallow reservoir.
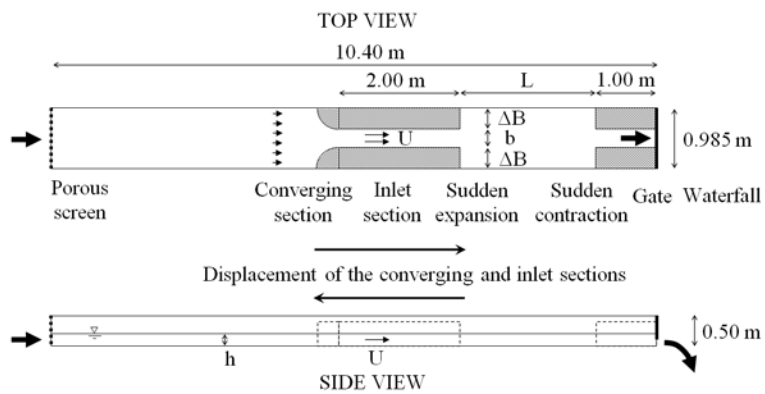
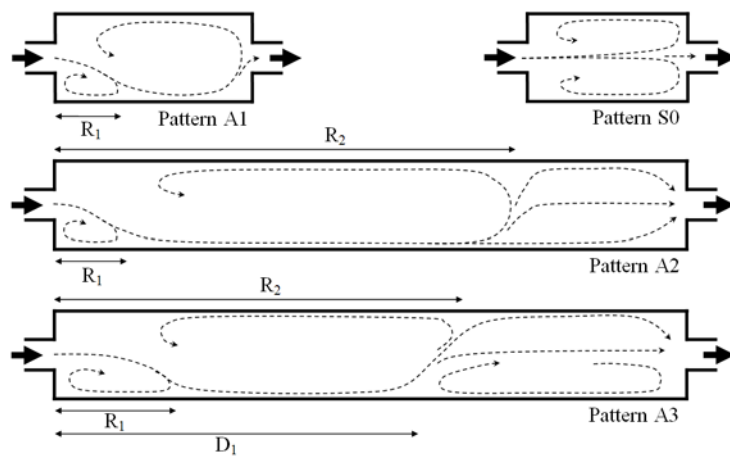Fig. 2. Sketch of the experimental set-up.

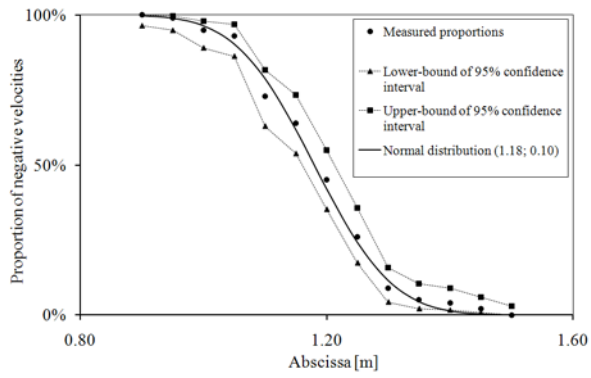Fig. 3. Schemes of the three stable flow patterns (not to scale).

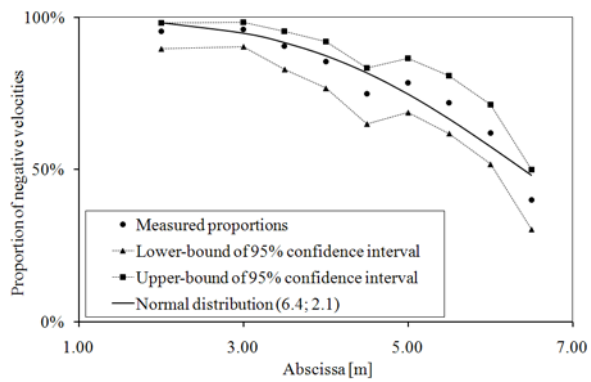Fig. 4. First reattachment of test F4-a.

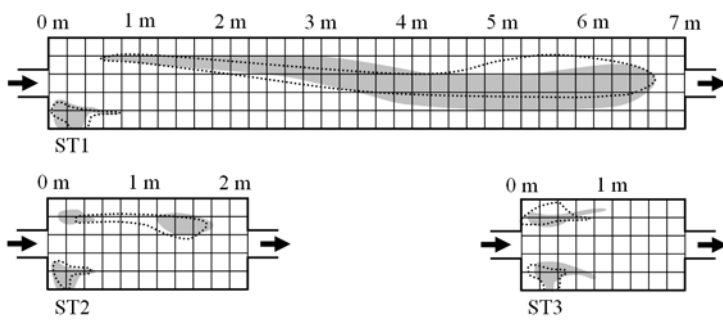Fig. 5. Second reattachment of test F4-c (the normal distribution is truncated).

Fig. 6. Experimental deposits on the bed of the reservoir (grey zones correspond to tests a; dotted lines, to tests b).
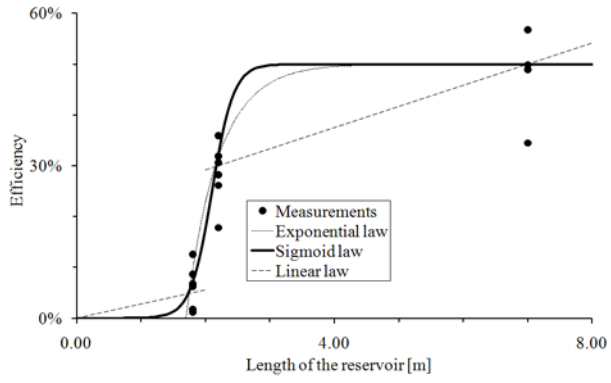
Fig. 7. Efficiency varying the length of the reservoir (parameters of the exponential law:

$\eta_0 = 50\%$, $\alpha = 2$ m^{-1}, $L_0 = 1.7$ m; sigmoid law: $\eta_0 = 50\%$, $\alpha = 6$ m^{-1}, $L_0 = 2.1$ m).